



states in doped  $V_2O_5$  nanowires facilitate fast ( $<500$  fs) hole transfer from CdSe QDs.<sup>22</sup> The authors propose that the resulting charge-separated state could be used to delay charge recombination and improve photocatalytic proton reduction.<sup>22,23</sup> In order to study homogeneous photocatalytic systems, we hypothesized that polyoxovanadate (POV) clusters could be used as an alternative to  $V_2O_5$  nanowires for efficient hole extraction. While most POV clusters are isolated in their most-oxidized state (*i.e.* electron-deficient), the polyoxovanadate-alkoxide (POV-alkoxide) clusters explored in this study (Fig. 1) are reduced analogues of these metal oxide assemblies, rendering them well-suited to serve as hole-transfer reagents in photocatalytic schematics (Fig. S1, ESI†).<sup>24</sup> Indeed, POV-alkoxide clusters have been shown to reductively quench molecular chromophores for reactions such as water oxidation.<sup>25</sup> However, they have not been studied in combination with QD photosensitizers.

To test our hypothesis that charge transfer between photoexcited CdSe QDs and the POV-alkoxide cluster,  $[V_6O_7(OC_2H_5)_{12}]^{1-}$ , is possible, steady-state photoluminescence quenching experiments were conducted. Given previous activity of mid-sized CdSe QDs as photocatalysts, QDs with a first excitonic absorbance peak at 525 nm ( $\pm 5$  nm) (correlating with a diameter of approximately 2.6 nm<sup>26</sup>) capped with trioctylphosphine (TOP) ligands were synthesized (Fig. S2, ESI†).<sup>27</sup> Their luminescence was monitored in the presence of increasing equivalents of  $[V_6O_7(OC_2H_5)_{12}]^{1-}$  (Fig. 2 inset). The photoluminescence of the QDs was efficiently quenched in the presence of the POV-alkoxide clusters, with a 96% decrease in emission intensity at 10 equivalents. The nonlinear behavior of the Stern–Volmer analysis suggests that the clusters quench the QD fluorescence through both static and dynamic mechanisms (Fig. S3, ESI†).<sup>28</sup> It is worth noting that there is a small overlap between the absorbance spectrum of  $[V_6O_7(OC_2H_5)_{12}]^{1-}$  and the emission of CdSe QDs, so we cannot definitively rule out the possibility of

an energy transfer quenching mechanism (Fig. 2). However, given the low absorbance of the clusters at these concentrations, contributions from such a pathway are predicted to be negligible in comparison to those of charge transfer (Fig. S4; see ESI† for details).

Given the promising results from photoluminescence quenching (*vide supra*), we sought to probe the proton reduction characteristics upon the addition of  $[V_6O_7(OC_2H_5)_{12}]^{1-}$  to a solution of glutathione-capped (CdSe–GSH) QDs and sacrificial electron donor ascorbic acid (Fig. 3). For this study, we opted to not include an external co-catalyst in an effort to simplify the already-complicated system, ensuring that any changes in catalysis were due to cluster/QD interactions. To establish a baseline for photoactivity of QDs under our conditions, a mixture of ascorbic acid and CdSe–GSH QDs, dissolved in ethanol and water (1 : 1), was irradiated with green (530 nm  $\pm$  10 nm) light (Fig. 3 and Fig. S5, ESI†). Over 48 hours, the multicomponent system produces 110  $\mu$ mol ( $\pm 42$   $\mu$ mol) of  $H_2$ . In the absence of ascorbic acid, negligible hydrogen evolution is observed (Fig. S6, ESI†). The rate of  $H_2$  evolution remains constant over this time frame, indicating minimal degradation of the QDs, with an average rate of  $H_2$  evolution of 2.22  $\mu$ mol  $h^{-1}$  ( $\pm 0.78$   $\mu$ mol  $h^{-1}$ ). This correlates to a quantum yield (QY) of 8.0% ( $\pm 2.4\%$ ) (see ESI† for details).

Upon addition of  $[V_6O_7(OC_2H_5)_{12}]^{1-}$  (100  $\mu$ M) to the photocatalytic system described above, both the average  $H_2$  evolved in 48 hours and the rate of catalysis are approximately doubled (Fig. 3 and Fig. S5, ESI†). The total  $H_2$  produced improves to 222  $\mu$ mol ( $\pm 37$   $\mu$ mol) with an improvement in rate to 4.61  $\mu$ mol  $h^{-1}$  ( $\pm 0.85$   $\mu$ mol  $h^{-1}$ ), and an increase of 125% in average QY to 18% ( $\pm 4.5\%$ ). To evaluate whether  $[V_6O_7(OC_2H_5)_{12}]^{1-}$  might act as a  $H_2$ -production catalyst, which would complicate its intended use as an electron mediator in this system, independent electrochemical analysis of the POV-alkoxide cluster was performed. Upon titration of 40 mM aqueous phosphate buffer (pH = 6) to a solution of 1 mM  $[V_6O_7(OC_2H_5)_{12}]^{1-}$  and 0.1 M  $[^nBu_4N]PF_6$  in acetonitrile, no change in the electrochemical response of the cluster was observed, indicating that this reduced POV-alkoxide cluster is not active as a proton reduction catalyst (Fig. S7, ESI†). Taken together, these results support our hypothesis that POV-alkoxide clusters efficiently extract the hole from CdSe QDs, acting as a hole shuttle and resulting in improved production of  $H_2$ .

Activity enhancement from the introduction of the POV-alkoxide cluster to the GSH-capped CdSe QDs prompted further exploration of the photocatalytic system. Given previously reported ligand-dependence on the photocatalytic activity of QDs,<sup>12,29–31</sup> additional thiolate ligands were selected to determine if the mechanism of enhancement by  $[V_6O_7(OC_2H_5)_{12}]^{1-}$  could be generalized to other QD-ligand systems. Cysteine (Cys) and 3-mercaptopropionic acid (MPA) were chosen as additional water-soluble ligands to cap QDs (Fig. 3A and Fig. S8, ESI†). The impact of the capping ligands on the first excitonic absorbance is small ( $<10$  nm).

It has been previously reported that the degree of passivation of surface  $Cd^{2+}$  ions dramatically influences the yield of proton reduction for QDs in the absence of a co-catalyst.<sup>8,32,33</sup>

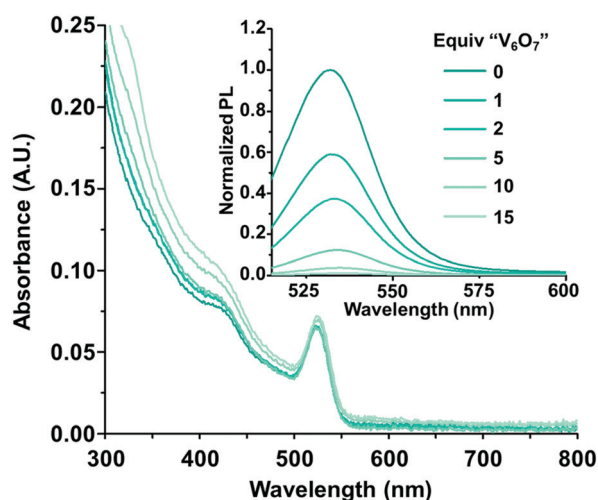
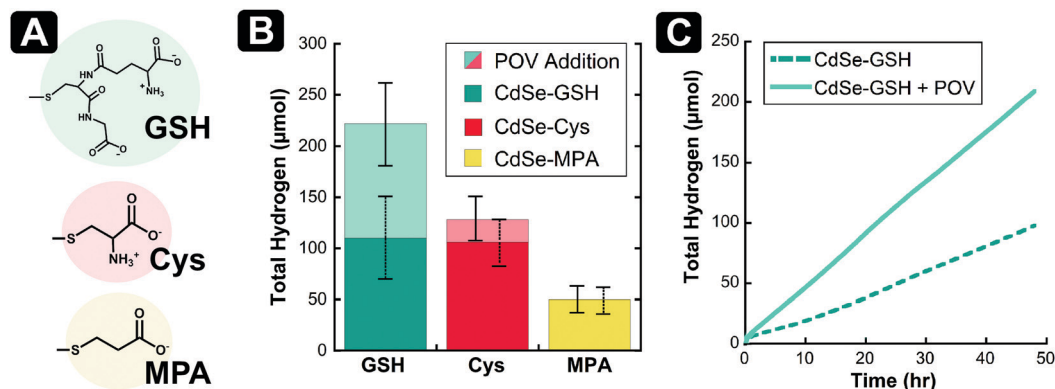


Fig. 2 The absorbance and photoluminescence (inset) spectra of CdSe–TOP with varying equivalents of  $[V_6O_7(OC_2H_5)_{12}]^{1-}$  (“ $V_6O_7$ ”). All samples contained 1  $\mu$ M CdSe with 0–15 equivalents of  $[V_6O_7(OC_2H_5)_{12}]^{1-}$  in dichloromethane and the photoluminescence was normalized to the absorbance at the excitation wavelength (500 nm).



**Fig. 3** (A) Structures of the capping ligands used on the surface of CdSe QDs; (B) total H<sub>2</sub> evolution after 48 hours from CdSe-GSH, CdSe-Cys, and CdSe-MPA in the presence of 0.5 M ascorbic acid, in a 1:1 EtOH:H<sub>2</sub>O mixture, being irradiated by 530 nm light at 15 °C. Upon addition of 100 μM [V<sub>6</sub>O<sub>7</sub>(OC<sub>2</sub>H<sub>5</sub>)<sub>12</sub>]<sup>1-</sup>, the positive change in total H<sub>2</sub> production for CdSe-GSH and CdSe-Cys is shown (*n* = 3); (C) representative trials of H<sub>2</sub> evolution over time for the CdSe-GSH H<sub>2</sub> evolution system described in (B), showing improvement in the presence of [V<sub>6</sub>O<sub>7</sub>(OC<sub>2</sub>H<sub>5</sub>)<sub>12</sub>]<sup>1-</sup>.

Given the differences in the molecular structure of the three thiolate ligands investigated in this work, we anticipated that surface coverage would vary between GSH-, Cys- and MPA-capped QDs. Thus, to establish new baselines for H<sub>2</sub> production for each system, we evaluated the photocatalysis for the CdSe QDs in the absence of POV-alkoxide clusters. The CdSe-Cys and CdSe-MPA systems have slow H<sub>2</sub> evolution in the first ten hours of catalysis (Fig. S9 and S10, ESI†). After this induction period, H<sub>2</sub> generation is linear over the remainder of the experiment. This is in contrast to the GSH-capped QDs, which produce H<sub>2</sub> at a constant rate throughout the 48 hours of irradiation (Fig. 3C). In total, the Cys-capped CdSe QDs produce a similar amount of H<sub>2</sub> to those capped with glutathione ligands (106 μmol ± 22 μmol), while the CdSe-MPA analogues produce significantly less H<sub>2</sub> in the same time period (50 μmol ± 12 μmol) (Fig. S11, ESI†). Since proton reduction has been reported to occur at solvated Cd surface-sites,<sup>8</sup> these differences in H<sub>2</sub> production without POV-alkoxide clusters suggest that MPA-capped QDs have a higher packing density than Cys- or GSH-capped QDs. This may be due to differences in the available binding modes of the ligands, or the ligand exchange procedures used.

Upon introduction of [V<sub>6</sub>O<sub>7</sub>(OC<sub>2</sub>H<sub>5</sub>)<sub>12</sub>]<sup>1-</sup> to the photocatalytic experiments with Cys- and MPA-capped QDs, interesting trends were observed. As with GSH, Cys-capped CdSe QDs showed a boost in activity with the addition of POV-alkoxide clusters (Fig. 3 and Fig. S9, ESI†). In the presence of clusters, the average H<sub>2</sub> evolved increases to 128 μmol (±20 μmol) from 106 μmol (±22 μmol). In contrast, negligible change in the total production of H<sub>2</sub> is observed upon addition of POV-alkoxide cluster to the MPA-capped CdSe QDs (Fig. 3 and Fig. S10, ESI†; 50 μmol ± 12 μmol vs. 48 μmol ± 10 μmol with [V<sub>6</sub>O<sub>7</sub>(OC<sub>2</sub>H<sub>5</sub>)<sub>12</sub>]<sup>1-</sup>).

We justify the observed differences in H<sub>2</sub> production as resulting from differences in the interactions between the QDs and the POV-alkoxide clusters. The ligands chosen to probe the photocatalytic reactivity of these QDs have a different charge at pH = 4.5, thus providing a different surface chemistry for the photosensitizer. Glutathione is a zwitterionic tripeptide containing cysteine, glutamate, and glycine (pK<sub>a</sub>s: 2.1 (COOH),

3.5 (COOH), 8.8 (NH<sub>3</sub><sup>+</sup>)). It is anticipated that this ligand binds to the surface of the QD through the thiol moiety, allowing for the remaining charged regions of the ligand to interact with the environment.<sup>34</sup> At pH = 4.5, the amine group located on the GSH ligand will remain protonated (*i.e.* positively-charged) and may interact with the anionic charge-states of the POV-alkoxide cluster.<sup>35</sup> As charge transfer from the POV-alkoxide to the QD occurs, the anionic cluster cycles through higher oxidation states (*e.g.* [V<sub>6</sub>O<sub>7</sub>(OC<sub>2</sub>H<sub>5</sub>)<sub>12</sub>]<sup>*n*</sup>; *n* = 0, 1+, 2+), at which point the charge attraction with the amine group becomes less favorable. The diminished coulombic interaction between the anionic POV-alkoxide cluster and the positively charged residues at the QD surface drives more oxidized forms of the cluster away from the QD surface, preventing charge recombination *via* back electron transfer. The dissociated, oxidized form of the POV-alkoxide cluster subsequently reacts with ascorbic acid, resulting in re-reduction of the vanadium oxide assembly.

Supporting this mechanistic hypothesis, photocatalytic experiments with CdSe-Cys dots also showed an increase in the amount of H<sub>2</sub> produced in the presence of [V<sub>6</sub>O<sub>7</sub>(OC<sub>2</sub>H<sub>5</sub>)<sub>12</sub>]<sup>1-</sup>. Cysteine, an amino acid (pK<sub>a</sub>s: 1.8 (COOH), 10.7 (NH<sub>3</sub><sup>+</sup>)), has also been used as a zwitterionic capping ligand for QDs.<sup>12,36</sup> The cysteine ligands offer a similar positively charged site for electrostatic interactions to occur, attracting the reduced cluster to the surface of the QD. We believe, however, that the smaller size of cysteine relative to glutathione leads to a more densely packed surface which inhibits the adsorption of [V<sub>6</sub>O<sub>7</sub>(OC<sub>2</sub>H<sub>5</sub>)<sub>12</sub>]<sup>1-</sup>, reducing the impact the clusters have on catalysis.

In contrast, CdSe-MPA showed no enhancement of H<sub>2</sub> production in the presence of [V<sub>6</sub>O<sub>7</sub>(OC<sub>2</sub>H<sub>5</sub>)<sub>12</sub>]<sup>1-</sup>. The absence of a positively charged residue in the MPA capping ligands would disfavor interaction between the QD and the reduced, anionic forms of the POV-alkoxide cluster. Instead, the more oxidized (cationic) states of the POV-alkoxide cluster (*e.g.* [V<sub>6</sub>O<sub>7</sub>(OC<sub>2</sub>H<sub>5</sub>)<sub>12</sub>]<sup>*n*</sup>; *n* = 1+, 2+) would be attracted to the QD surface. In these oxidation states, the cluster would energetically prefer to accept reducing equivalents from the QD, no longer functioning as a hole scavenging reagent. Also, as noted above, MPA-capped CdSe QDs appear

to have fewer uncoordinated sites, which could further inhibit interaction with the POV-alkoxide clusters and hole transfer from the QD.

Here, we have used POV-alkoxide clusters to efficiently extract photogenerated holes from CdSe QDs in order to significantly increase the volume of H<sub>2</sub> produced without the addition of a proton reduction co-catalyst. CdSe QDs capped with GSH show the largest increase in both the rate of reaction and the total amount of H<sub>2</sub> produced with the addition of POV-alkoxide clusters. Cys-capped QDs show a moderate increase in the amount of H<sub>2</sub> produced when clusters are present, while QDs capped with MPA show no significant increase in the amount of H<sub>2</sub> produced following addition of the vanadium oxide cluster. These results provide insight into the electrostatic interaction required for charge transfer between the photosensitizer and the cluster, which will aid in designing more efficient systems for the photocatalytic production of H<sub>2</sub>.

This work is supported by the Chemical Sciences, Geosciences and Biosciences Division, Office of Basic Energy Sciences, Office of Science, U.S. Department of Energy, Grant No. DE-FG02-09ER16121. E. H. E. Acknowledges support from NIH training grant T32-GM118283.

## Conflicts of interest

There are no conflicts to declare.

## Notes and references

- 1 C. Huang, X.-B. Li, C.-H. Tung and L.-Z. Wu, *Chem. – Eur. J.*, 2018, **24**, 11530–11534.
- 2 M. S. Kodaimati, K. P. McClelland, C. He, S. Lian, Y. Jiang, Z. Zhang and E. A. Weiss, *Inorg. Chem.*, 2018, **57**, 3659–3670.
- 3 R. D. Harris, S. Bettis Homan, M. Kodaimati, C. He, A. B. Nepomnyashchii, N. K. Swenson, S. Lian, R. Calzada and E. A. Weiss, *Chem. Rev.*, 2016, **116**, 12865–12919.
- 4 D. J. Norris and M. G. Bawendi, *Phys. Rev. B: Condens. Matter Mater. Phys.*, 1996, **53**, 16338–16346.
- 5 J. Barber, *Chem. Soc. Rev.*, 2009, **38**, 185–196.
- 6 T. R. Cook, D. K. Dogutan, S. Y. Reece, Y. Surendranath, T. S. Teets and D. G. Nocera, *Chem. Rev.*, 2010, **110**, 6474–6502.
- 7 X.-B. Li, C.-H. Tung and L.-Z. Wu, *Nat. Rev. Chem.*, 2018, **2**, 160–173.
- 8 J. Zhao, M. A. Holmes and F. E. Osterloh, *ACS Nano*, 2013, **7**, 4316–4325.
- 9 V. V. Matyilitsky, L. Dworak, V. V. Breus, T. Basché and J. Wachtveitl, *J. Am. Chem. Soc.*, 2009, **131**, 2424–2425.
- 10 F. F. Schweinberger, M. J. Berr, M. Döblinger, C. Wolff, K. E. Sanwald, A. S. Crampton, C. J. Ridge, F. Jäckel, J. Feldmann, M. Tschurl and U. Heiz, *J. Am. Chem. Soc.*, 2013, **135**, 13262–13265.
- 11 M. J. Berr, F. F. Schweinberger, M. Döblinger, K. E. Sanwald, C. Wolff, J. Breimeier, A. S. Crampton, C. J. Ridge, M. Tschurl, U. Heiz, F. Jäckel and J. Feldmann, *Nano Lett.*, 2012, **12**, 5903–5906.
- 12 E. A. Weiss, *ACS Energy Lett.*, 2017, **2**, 1005–1013.
- 13 Z. Han, F. Qiu, R. Eisenberg, P. L. Holland and T. D. Krauss, *Science*, 2012, **338**, 1321–1324.
- 14 K. E. Knowles, M. D. Peterson, M. R. McPhail and E. A. Weiss, *J. Phys. Chem. C*, 2013, **117**, 10229–10243.
- 15 P. V. Kamat, J. A. Christians and J. G. Radich, *Langmuir*, 2014, **30**, 5716–5725.
- 16 S. Lian, D. J. Weinberg, R. D. Harris, M. S. Kodaimati and E. A. Weiss, *ACS Nano*, 2016, **10**, 6372–6382.
- 17 R. D. Harris, V. A. Amin, B. Lau and E. A. Weiss, *ACS Nano*, 2016, **10**, 1395–1403.
- 18 J. R. Lee, W. Li, A. J. Cowan and F. Jäckel, *J. Phys. Chem. C*, 2017, **121**, 15160–15168.
- 19 O. M. Pearce, J. S. Duncan, N. H. Damrauer and G. Dukovic, *J. Phys. Chem. C*, 2018, **122**, 17559–17565.
- 20 C. M. Wolff, P. D. Frischmann, M. Schulze, B. J. Bohn, R. Wein, P. Livadas, M. T. Carlson, F. Jäckel, J. Feldmann, F. Würthner and J. K. Stolarczyk, *Nat. Energy*, 2018, **3**, 862–869.
- 21 T. X. Ding, J. H. Olshansky, S. R. Leone and A. P. Alivisatos, *J. Am. Chem. Soc.*, 2015, **137**, 2021–2029.
- 22 J. Cho, A. Sheng, N. Suwandaratne, L. Wangoh, J. L. Andrews, P. Zhang, L. F. J. Piper, D. F. Watson and S. Banerjee, *Acc. Chem. Res.*, 2019, **52**, 645–655.
- 23 J. L. Andrews, J. Cho, L. Wangoh, N. Suwandaratne, A. Sheng, S. Chauhan, K. Nieto, A. Mohr, K. J. Kadassery, M. R. Popeil, P. K. Thakur, M. Sfeir, D. C. Lacy, T.-L. Lee, P. Zhang, D. F. Watson, L. F. J. Piper and S. Banerjee, *J. Am. Chem. Soc.*, 2018, **140**, 17163–17174.
- 24 L. E. VanGelder, A. M. Kosswattaarachchi, P. L. Forrestel, T. R. Cook and E. M. Matson, *Chem. Sci.*, 2018, **9**, 1692–1699.
- 25 M.-P. Santoni, G. La Ganga, V. Mollica Nardo, M. Natali, F. Puntoriero, F. Scandola and S. Campagna, *J. Am. Chem. Soc.*, 2014, **136**, 8189–8192.
- 26 W. W. Yu, L. Qu, W. Guo and X. Peng, *Chem. Mater.*, 2003, **15**, 2854–2860.
- 27 F. Qiu, Z. Han, J. J. Peterson, M. Y. Odoi, K. L. Sowers and T. D. Krauss, *Nano Lett.*, 2016, **16**, 5347–5352.
- 28 J. R. Lakowicz, in *Principles of Fluorescence Spectroscopy*, ed. J. R. Lakowicz, Springer, US, Boston, MA, 2006, pp. 277–330, DOI: 10.1007/978-0-387-46312-4\_8.
- 29 A. Das, Z. Han, M. G. Haghghi and R. Eisenberg, *Proc. Natl. Acad. Sci. U. S. A.*, 2013, **110**, 16716–16723.
- 30 C. M. Chang, K. L. Orchard, B. C. M. Martindale and E. Reisner, *J. Mater. Chem. A*, 2016, **4**, 2856–2862.
- 31 M. Green, *J. Mater. Chem.*, 2010, **20**, 5797–5809.
- 32 M. J. Greaney, E. Couderc, J. Zhao, B. A. Nail, M. Mecklenburg, W. Thornbury, F. E. Osterloh, S. E. Bradforth and R. L. Brutchey, *Chem. Mater.*, 2015, **27**, 744–756.
- 33 W. D. Kim, J.-H. Kim, S. Lee, S. Lee, J. Y. Woo, K. Lee, W.-S. Chae, S. Jeong, W. K. Bae, J. A. McGuire, J. H. Moon, M. S. Jeong and D. C. Lee, *Chem. Mater.*, 2016, **28**, 962–968.
- 34 P. K. Sudeep, S. T. S. Joseph and K. G. Thomas, *J. Am. Chem. Soc.*, 2005, **127**, 6516–6517.
- 35 Z. Aliakbar Tehrani, Z. Jamshidi, M. Jebeli Javan and A. Fattahi, *J. Phys. Chem. A*, 2012, **116**, 4338–4347.
- 36 F. Shi, S. Liu and X. Su, *New J. Chem.*, 2017, **41**, 4138–4144.